Physical Modelling in Geotechnics

Centrifuge model tests on the effects of the supporting dense sand layer thickness on a pile under static loading

I.G. Martinez, R. Kido & M. Kimura
Department of Civil and Earth Resources Engineering, Kyoto University, Kyoto, Japan

Y. Sawamura
Department of Urban Management, Kyoto University, Kyoto, Japan

ABSTRACT: End-bearing piles resist loads primarily through the end-bearing resistance from contact with the bedrock or a dense sand layer. In areas where the dense sand layer thickness is unable to satisfy conventional design requirements, the piles are designed as friction piles, which may be uneconomical. Thus, it is necessary to investigate the effects of the bearing layer thickness on the pile bearing characteristics. Centrifuge model tests (50G) were conducted to observe the response of the pile and the soil surrounding the pile tip during static loading. Five cases were conducted with varying bearing layer thickness-to-pile diameter ratios (H/D): 0, 1, 2, 3, and 8. The dense sand layer was composed of dry Silica sand No. 5 (Dr = 90%,), while the underlying soil layer was modeled using dry Toyoura sand (Dr = 20-30%). Load-displacement curves and lateral earth pressure data showed that bearing characteristics of the case with H/D = 3 and H/D = 8 are similar, suggesting that the ultimate total bearing capacity of a dense sand layer with a thickness of 3D can be assumed to be equal to that of a full bearing layer.

Keywords: centrifuge modeling, pile foundation, static loading, sand, lateral earth pressure

1 INTRODUCTION

End-bearing piles resist loads primarily through contact with the bedrock or a dense sand layer, in cases where the bedrock is located at a large depth. The properties and thickness of this dense sand layer are dictated by local design codes. If these requirements are not met, the piles are designed as friction piles, which may be uneconomical as they extend to greater depths to achieve the required resistance.

In areas such as the Osaka Bay Area, the ground consists of alternating dense sand and soft clay layers (Oda and Takegawa, 2014). These dense sand layers may provide enough resistance to be considered as a bearing layer. However, current design codes may require the piles to be designed as friction piles due to the relatively low thickness of these layers. Therefore, it is necessary to investigate the effects of the dense sand layer thickness on the bearing characteristics of the pile. By doing so, the design of the pile may be optimized in consideration of the ground conditions.

Displacement field analysis through X-ray CT has been performed to investigate the influence zone of a pile supported by a bearing layer of various thicknesses (Suezawa *et al.*, 2020). The influence zone was found to have a bulb shape, with a cone of high displacement directly below the pile tip. In addition, through a finite element method (FEM) analysis, the failure mechanism of a pile supported by a thin bearing layer has been described to be a punching shear failure (Oda and Takegawa, 2014). Failure initiates at the edges of the pile and in the underlying soil layer, which eventually come into contact, resulting in the failure of the pile. Centrifuge studies have also been performed to determine the relationship between the end bearing capacity of the pile and the bearing layer thickness (Horii and Nagao, 2018). For thin bearing layers, the end bearing capacity can be determined using the equation used for calculating the capacity of a pile in a two-layered ground (with underlying clay layer). The spread angle, or the angle of the influence area, was determined to be 23° for a thin bearing layer underlain by saturated clay. While these studies have characterized the behavior of a thin bearing layer, there have been limited studies on the general effects of the bearing layer thickness on the bearing mechanism.

Considering the above, the objective of the present study is to determine the effect of the bearing layer thickness on the bearing mechanism of the pile through centrifuge model tests. The focus of the study is to determine the effects on the load-displacement curves, the axial load distribution, and the lateral earth pressure in the soil surrounding the pile tip.

2 METHODOLOGY

The centrifuge model tests were conducted under an acceleration of 50G in the Geotechnical Centrifuge Center of the Disaster Prevention Research Institute (DPRI) of Kyoto University.

To determine the effects of the bearing layer thickness on the pile behavior, a total of eight (8) tests were conducted. Five (5) corresponded to 5 cases with different bearing layer thicknesses (H): Case-0D, Case-1D, Case-2D, Case-3D, and Case-8D, where D is the pile diameter. The last three (3) tests were conducted on cases where H = 1D, 3D, and 8D, with earth pressure gauges (EPG) positioned in the soil to measure the lateral earth pressure. These are hereafter referred to as Case-1D-EPG, Case-3D-EPG, and Case-8D-EPG.

2.1 Model Pile

The model pile used in the study was a stainless steel pipe (SUS304), with a Young's Modulus of 139 GPa, a diameter of 20 mm, and a length of 200 mm in model scale. Steel caps were placed at the ends to model a closed-ended pile. Six pairs of strain gauges (Type FLA-2-23-3LHT, Tokyo Measuring Instruments Laboratory, Co., Ltd.) were used to determine the axial load distribution along the pile. The pile and the positions of the strain gauges are presented in Fig. 1.

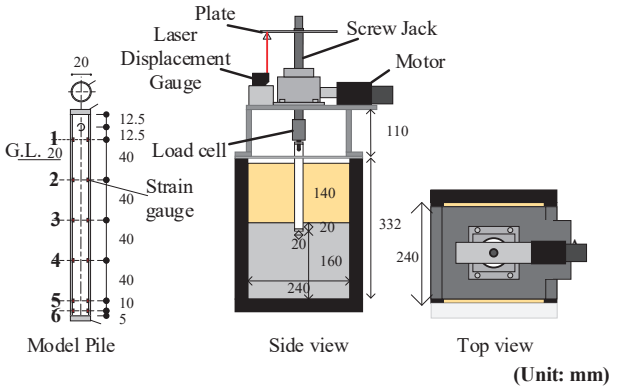

Fig. 1. Model pile and experimental set up.

2.2 Soil Materials

The bearing layer, or the dense sand layer, was composed of Silica sand No. 5 with a relative density of D_r = 90%, while the underlying and the upper layers were composed of Toyoura sand (D_r = 20% for the underlying layer and 30% for the upper friction layer). The difference in the relative density of the upper and lower loose layers were determined considering the possible densification of the underlying sand during model preparation. In this study, dry sand was considered to simplify the model and to determine the effects of the soil material and hydraulic conditions through comparison with the results of the centrifuge model test performed by the previous study. These sand materials were chosen for this study considering the particle size effect and the achievable relative density through air pluviation. Table 1 shows the soil properties.

Table 1. Soil properties.

	Toyoura sand	Silica sand No. 5
Specific Gravity G_s	2.640	2.640
D_{50} [mm]	0.200	0.438
Min. Void Ratio e_{min}	0.585	0.699
Max. Void Ratio e_{max}	0.975	0.961
Cohesion c [kPa]	0	0
Friction Angle ϕ [deg]	33.4	33.0

2.3 Model Preparation

The models were prepared using air pluviation to preserve the low relative density of the underlying sand layer. After constructing the bottom 8D soil layers, the pile was placed on top of the soil and the remaining soil layers were constructed. Thus, initial stresses from pile installation may be assumed to be negligible.

For the three (3) tests with the earth pressure gauges, two pairs of 3-MPa gauges (PDA-3MPB, Tokyo Measuring Instruments Laboratory Co., Ltd.) were placed in the soil beneath the pile tip. One pair was positioned 1D below the pile tip, while the other at 2D below the tip. For each pair, one gauge was placed 0.50D from the pile edge, while the other at 0.75D from the edge. Fig. 2 shows the position of the earth pressure gauges. To accurately measure the lateral earth pressure, it must be ensured that the gauges remain in the same position throughout loading. Thus, the earth pressure gauges were attached to supports made of aluminum bars. These were then attached to the walls of the soil chamber using adhesive, which was ensured to provide sufficient support such that the bars were not detached from the soil chamber walls after the experiment. Moreover, the bars were supported by the soil layers beneath it, particularly around the soil chamber walls.

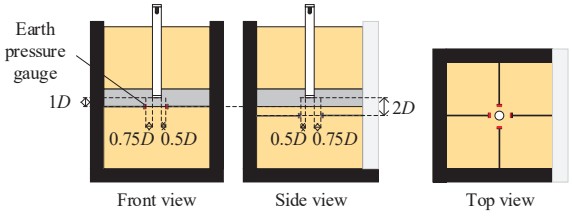

Fig. 2. Position of earth pressure gauges.

2.4 Testing Procedure

Once the model had been prepared, displacement gauges, a 5-kN load cell (TCLN-5KNA Tension/Compression Load Cell, Tokyo Measuring Instruments Laboratory, Co., Ltd.), and a screw jack (J1GLUK0100NSN, Nippon Gear Co., Ltd.) were positioned, as shown in Fig. 1. The model was then

placed in the centrifuge and the acceleration was increased. Once the centrifugal acceleration reached 50G, the screw jack was remotely controlled to displace the pile head with a rate of 0.01 mm/min (model scale) until a vertical displacement of 1.0D had been reached. The vertical displacement of the pile was measured using a 65-mm laser displacement gauge (IL Laser Sensor IL-065, Keyence Co., Ltd.), while two other laser displacement gauges were used to measure the horizontal displacement of the pile to ensure that the pile moved only in the vertical direction. Once the static load test was completed, the centrifuge was decelerated.

3 RESULTS

3.1 Load-Displacement Curves and End Bearing Capacity

Figure 3 shows the relationship between the pile head load and the pile head displacement normalized by the pile diameter. The values increase with the bearing layer thickness when the bearing layer thickness ranges from 0D-3D. However, once the bearing layer thickness exceeds 3D, there are no significant changes, particularly at low pile displacements. As the bearing capacity of the pile is taken as the total load corresponding to a pile head displacement of 0.1D, it can be concluded from the load-displacement curve that a bearing layer thickness of at least 3D can be treated as a full bearing layer.

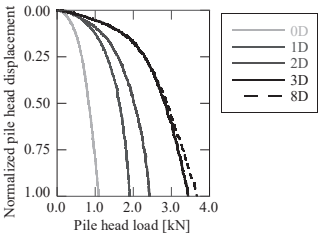

Fig. 3. Load-displacement curves.

3.2 Axial Load Distribution

Figure 4 shows the axial load distribution along the pile at pile head displacements equal to 0.010D, 0.025D, 0.050D, and 0.100D. Despite both points being located above the ground, the pile head (load cell) and the first strain gauge have different axial load values. This may be due to gauge factors and the absorption of the load at the contact point between the steel cap and the steel pipe. Nonetheless, the axial load distribution along the pile can be analyzed from the strain gauge measurements.

Similar tendencies were observed for all cases, with the curves generally characterized by three segments: (1) a slight decrease between the 1st and 2nd pair of gauges, particularly for thicker bearing layers, (2) nearly constant values from the 2nd to the 4th gauge, and (3) a significant decrease between the 5th and 6th gauges. These suggest that frictional resistance along the pile shaft mainly acts in the region of the pile embedded in the bearing layer. At low pile displacements, the axial load distribution is similar for all cases. This may be attributed to the displacements at which the shaft resistance and the end bearing resistance are mobilized. As the shaft resistance is known to mobilize at lower displacements, the similar ground model along the pile shaft for all cases results in similar axial load distributions. As the pile displacement increases, the discrepancy among the cases increases. These suggest that in the current model, the pile capacity is largely dependent on the end bearing resistance and is therefore able to exhibit the effects of the bearing layer thickness on the pile bearing mechanism.

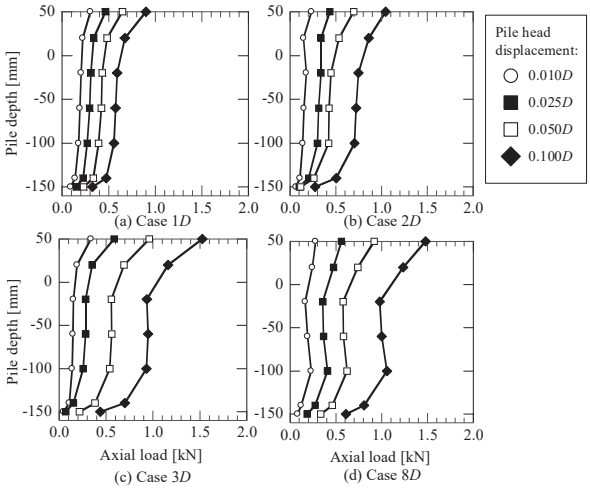

Fig. 4. Axial load distribution.

3.3 End Bearing Capacity

Figure 5 shows the relationship between the end bearing capacity and the thickness-to-pile diameter ratio, compared with the equation used by Horii and Nagao (2018) for a bearing layer underlain by saturated clay:

$$q_p = \left(1 + 2\,{}^{H}/_{D}\,\tan\theta\right)^2 q_l \qquad (1)$$

where q_p is the end bearing capacity, θ is the spread angle, and q_l is the bearing capacity of the lower layer.

Using the end bearing capacity of Case-0D in the equation largely overestimates the end bearing capacity, while the best fit curve largely underestimates the bearing capacity of Case-1D. This suggests that the equation cannot be directly applied to the dry sand model in this study.

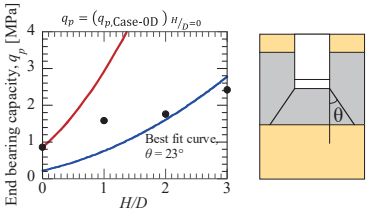

Fig. 5. End bearing capacity.

3.4 Lateral Earth Pressure

Figure 6 shows the relationship between the pile head displacement and the lateral earth pressure from the four (4) gauges for each case. It must be noted that the method by which the earth pressure gauges were positioned may affect the values obtained. Nonetheless, considering the constant experimental set-up for all three cases and the consistencies in the trends observed from the curves, the relative values between the cases may be utilized in analyzing the effects on the lateral earth pressure.

The curves from the earth pressure gauges located 1*D* below the pile tip can be characterized by three stages: (1) an initial increase from a pile head displacement of 0.00 to 0.25*D*, (2) an intermediate region from 0.25 to 0.75*D*, and (3) a final decrease from 0.75 to 1.0*D*. On the other hand, the curves from the gauges located 2*D* below the pile tip increase throughout loading. These suggest that the soil around the gauges located 1*D* below the pile tip behaves elasto-plastically, while that around the gauges 2*D* below behaves elastically throughout loading.

The elasto-plastic behavior of the soil around the gauges 1*D* below the tip suggests an initial outward movement. After the yield point, the lateral earth pressure becomes constant, suggesting that the soil moves downward, parallel to the gauges, while applying a constant (lateral) pressure. This yield point was found to be consistent with the load-displacement curves. Strain softening then occurs, suggesting that the lateral movement of the soil is reduced, and the entire soil mass is moving downward with the pile.

While generally similar tendencies were observed for all cases, the values of the lateral earth pressure increase as the bearing layer thickness increases. This suggests that the region of high confining pressure is wider for a thicker bearing layer. Consequently, the region of large soil displacement is narrower for a thicker bearing layer. In addition to this, the difference between the lateral earth pressure at the two gauges located 1*D* below the pile tip was analyzed for all cases from a pile displacement of 0.00 to 0.25*D*. The difference was found to decrease as the bearing layer thickness increases. It is hypothesized that a smaller deviation suggests that both gauges (0.50 and 0.75*D* from pile edge) are located within the failure zone, while a larger deviation suggests that one gauge is closer to the boundary of the failure zone. The observations therefore suggest that a thicker bearing layer corresponds to a larger spread angle, with the failure zone encompassing both earth pressure gauges. This finding is consistent with the results of the displacement field analysis of the previous study (Suezawa *et al.*, 2020). With this, as the bearing layer thickness decreases, the spread angle decreases, and the soil becomes more dependent on the strength of the soil layers below the pile tip, thereby resulting in lower capacities. Furthermore, the smaller spread angle and the lower confining pressure further explain the rapid downward expansion of the failure zone which eventually results in a punching shear failure.

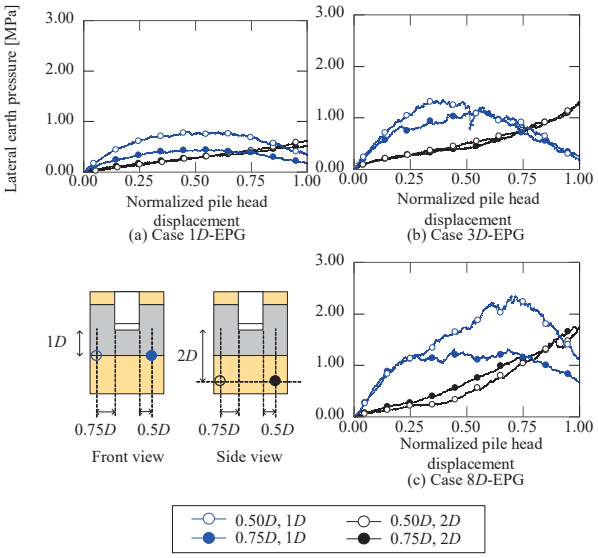

Fig. 6. Lateral earth pressure.

4 CONCLUSIONS

Centrifuge model tests were conducted to investigate the effect of the bearing layer thickness on the bearing mechanism of piles. It can be concluded that a bearing layer thickness of at least 3*D* can be treated as a full bearing layer. Moreover, the lateral earth pressure values suggest that the confining pressure and the spread angle increase as the bearing layer thickness increases. Therefore, for thin bearing layers, the pile is highly dependent on the strength of the soil layers directly below the pile tip. This then results in lower capacities and the punching shear failure observed in piles supported by thin bearing layers.

ACKNOWLEDGEMENTS

This research was supported by a grant “2019 年度阪神高速若手研究者助成” from Hanshin Expressway Co. Ltd.

REFERENCES

Horii, Y and Nagao, T. 2018. Centrifuge modelling of non-displacement piles on a thin bearing layer overlying a clay layer. *Physical Modelling in Geotechnics* 2(1): 1371-1376.

Oda, K. and Takegawa, S. 2014. Effect of stiffness of thin bearing layer on toe bearing mechanism of steel pipe pile with a concrete bulb, *International Journal of GEOMATE* 6(1): 763-770.

Suezawa, R., Kido, R., Sawamura, Y., and Kimura, M. 2020. Influence of bearing layer thickness on vertical bearing capacity of pile and soil deformation behavior, *Journal of Japan Society of Civil Engineers C (Geosphere Engineering)* 76(4): 429-440. (in Japanese)